Hindawi
Adsorption Science & Technology
Volume 2021, Article ID 4998706, 19 pages
https://doi.org/10.1155/2021/4998706

Research Article

Remediation of Cr(VI)/Cd(II)-Contaminated Groundwater with Simulated Permeable Reaction Barriers Filled with Composite of Sodium Dodecyl Benzene Sulfonate-Modified Maifanite and Anhydride-Modified Fe@SiO_2@Polyethyleneimine: Environmental Factors and Effectiveness

Jingqing Gao,[1] **Yalin Zhai**,[1] **Zhenzhen Huang**,[2] **Peng Ren**,[1] **Jianlei Gao**,[1] **Zhijun Chen**,[3] **and Shunling Li**[4]

[1]*School of Ecology and Environment, Zhengzhou University, Zhengzhou 450001, China*
[2]*School of Water Conservancy and Engineering, Zhengzhou University, Zhengzhou 450001, China*
[3]*School of Materials and Chemical Engineering, Zhengzhou University of Light Industry, Zhengzhou 450002, China*
[4]*Henan Jingu Environmental Protection Engineering Equipment, Zhengzhou 450000, China*

Correspondence should be addressed to Jingqing Gao; jingqinggao@zzu.edu.cn and Zhenzhen Huang; zzhuang@zzu.edu.cn

Received 16 June 2021; Revised 13 September 2021; Accepted 23 September 2021; Published 9 November 2021

Academic Editor: Muhammad Raziq Rahimi Kooh

A composite material of sodium dodecyl benzene sulfonate- (SDBS-) modified maifanite and anhydride-modified Fe@SiO_2@PEI (PEI) was used as an adsorbent for the removal of hexavalent chromium (Cr(VI)) and bivalent cadmium (Cd(II)) from groundwater by using column experiments and simulated PRB test. In this study, the optimum proportion of SDBS-modified maifanite and anhydride-modified Fe@SiO_2@PEI was 5 : 1. In the column experiments, it was found that the penetration time increased with the increase of the initial concentrations (30, 60, and 90 mg/L) and the decrease of the flow rates (5.45, 10.9, and 16.35 mL/min) at an influent pH of 6.5 ± 0.3. It was also obtained that the removal rates of Cr(VI) and Cd(II) reached 99.93% and 99.79% at an initial Cr(VI) and Cd(II) concentration of 30 mg/L with the flow rate of 10.9 mL/min, respectively, at 6 h. Furthermore, excellent removal effectiveness of Cr(VI) and Cd(II) (85.94% and 83.45%, respectively) was still achieved in simulated PRB test at a flow rate of 5.45 mL/min with the heavy metal solution concentration of 5.0 ± 0.5 mg/L (Cr(VI) and Cd(II) concentration were, respectively, 5.0 ± 0.5 mg/L); and the adsorbent had not completely failed by the end of the trial. Yoon-Nelson model was successfully applied to predict the breakthrough curves for the assessment of composite material heavy metal removal performance and was in good agreement with the experimental data of the heavy metal removal efficiency. The strong removal ability of the adsorbent could be attributed to the fact that maifanite with a large diameter can provide support and increase the permeability coefficient and porosity and that zero-valent iron (ZVI) can convert Cr(VI) to Cr(III) and improve the adsorption capacity of maifanite. The obtained results suggested that the novel PRB fillers have great significance for preventing and controlling Cr(VI)/Cd(II)-contaminated groundwater.

1. Introduction

Heavy metal pollution in groundwater has been a widespread environmental problem in recent years and could become a serious threat to human health and ecosystems. Compared to other metals in heavy metal-contaminated groundwater, chromium (Cr) and cadmium (Cd) are two of the most common heavy metals. And Cr and Cd were greatly concerned because of their abundance and toxicity even at very low concentrations. As an important raw material for industrial production, chromium is mainly used in leather, electroplating, dye, wood anticorrosion, and other industries. The unreasonable disposal of waste residue and wastewater containing chromium and the leaching of rainwater are among the main

reasons for increases in the concentration of chromium in groundwater [1]. Generally, chromium has two valence states, namely, Cr(VI) and trivalent chromium (Cr(III)), and its properties vary greatly due to its different valence states [2]. Cr(III) is less harmful and usually produces less soluble hydroxides. Compared with inert Cr(III), Cr(VI) is more unstable and 100 to 1000 times more toxic. Cadmium is a typical representative heavy metal, and its main sources include drainage sludge, landfill leachate, and mining waste from cadmium deposits. In addition, wastewater from nonferrous metal smelting enterprises, cadmium wastewater from the chemical industry, and the migration and settlement of atmospheric cadmium dust can all cause cadmium to enter water bodies. Cadmium is one of the most toxic and mobile elements in the environment, belonging to the "five poisons (cadmium, chromium, mercury, lead, arsenic, and their compounds)" [3]. In water environment, cadmium predominately exits in Cd(II) and moves mainly under aerobic and acidic conditions. Because Cd^{2+} and Ca^{2+} have similar ionic radii, the same charge, and similar chemical properties, they can replace calcium in minerals and accumulate in multiple organs of an organism. These effects can lead to structural and functional cell damage and even death. Due to their high solubility, portability, nonbiodegradability, and biological accumulation, Cr(VI) and Cd(II) may interfere with the ecosystem, damage human health, and cause serious environmental problems. Therefore, effective and economical techniques must be sought to remove Cr(VI) and Cd(II) from wastewater.

The site mainly involved in this study is a chromium and cadmium residue-contaminated field in northwestern Henan province; the Cr(VI) and Cd(II) concentration of contaminated groundwater here is up to a few hundred milligrams per liter [4]. Due to the high toxicity of the groundwater around here, it is very urgent and necessary to control the groundwater here, so a permeable reative barrier (PRB) is asked to be set to treat the contaminated groundwater around here.

PRB is a kind of pollution treatment technology that was proposed by the US Environmental Protection Agency in 1982 to intercept, block, and remediate contaminated plumes in situ. PRB is equipped with reactive media to separate contaminants from groundwater, does not require pumping and surface treatment systems, and consumes the internal reaction media more slowly. Accordingly, PRBs have several years or even decades of processing capacity and are highly competitive and economical. In previous studies, many reactive media have been used in PRB, such as ZVI, activated carbon, zeolite, lime, and other alkaline materials, as well as combinations of apatite, red mud, oxide, sodium disulfite, and reactive materials. To date, the materials used in PRBs have involved several techniques, including adsorption, chemical precipitation, membrane processes, ion exchange, sedimentation, biological treatment, electrodialysis, and reverse osmosis processes [5–7]. Most of these technologies have limitations, such as high cost, complex processing, and high energy consumption requirements, as well as the potential for secondary pollution [8, 9]. In these technologies, adsorption is the most practical approach due to its easy operation, low cost, high efficiency, and environmental friendliness. Traditional adsorbents (such as activated carbon, clay, and zeolite) [10, 11] are effective because of their high specific surface area (SSA), but they are not easy to get, expensive, inefficient, and difficult to separate from water and may cause secondary contamination. Hence, it is very important to choose adsorbents with low cost, wide sources, high efficiency, and environmental friendliness.

For a long time, the development of various iron-based reducing adsorbents into high removal efficiency in wastewater treatment has received international attention. Mallants et al. found that the removal of uranium was enhanced by ZVI by redox precipitation in PRB, and the average removal rate reached the highest value of 98% [12]. In another report, ZVI and zeolite were used as a PRB material and, combined with array electrodes (AEEK), efficiently remediated Cd(II) contaminated soil with a removal rate at 93.1% [13]. All these results revealed that ZVI played an important role in PRB. ZVI is a reductant which is highly reactive, inexpensive, and easy to separate and dispose. Its significant reduction potential (-440 mV) and strong precipitation capacity [14] hint of the possibility of attenuation and treatment of Cr(VI) and Cd(II). However, ZVI has its disadvantages related to easy oxidation and aggregation [15, 16], which limits its application.

Maifanite is a common mineral material with low cost, ready acquisition, and unique adsorption property [17]. Puls et al. (1999) applied maifanite modified with H_2SO_4 to remove nickel ions from groundwater. And the results showed that the maifanite obtained better adsorption of 90% [16]. Zhang et al. explored maifanite in constructed rapid infiltration systems (CRIS) to improve the adsorption performance of Cd(II) [18]. Gao et al. studied the removal of Cr(VI) by ZnAl-layered double hydroxides (LDHs) coated on maifanite substrate in CRIS. The experiments showed that maifanite/ZnAl-LDHs substrate displayed better Cr(VI) removal capacity induced by microorganism than that with natural maifanite [19]. Although maifanite has been well documented in the adsorption of heavy metal ions, all uses of maifanite have been limited to a single remediation material. It is noteworthy that it also presents a great potential to address the problem of the aggregation of ZVI due to its good mechanical properties and cavernous porosity [20].

Until now, no studies reported the application of the composite of ZVI and maifanite for removal of heavy metal-contaminated groundwater. Maifanite can be used as a heavy metal adsorption material, and it has good mechanical properties and porosity. ZVI has strong reducibility, but its application is limited due to its easy oxidation and agglomeration. The insertion of SDBS can increase the specific surface area of adsorbent and make its surface lamellar structure, so as to increase the permeable area of the solution, and then increase the adsorption capacity of the adsorbent and improve the adsorption rate. The groups including SiO_2, PEI, and anhydride can further improve the removal effect of heavy metals through group chelation. Therefore, we combined them on the basis of modification in this study,

which showed strong removal ability for Cr(VI) and Cd(II). The strong removal ability could be attributed to the fact that SDBS-modified maifanite with a large diameter can provide support and increase the permeability coefficient and porosity and that anhydride-modified Fe@SiO_2@PEI can convert Cr(VI) to Cr(III) and improve the adsorption capacity of maifanite.

Here, SDBS-modified maifanite and anhydride-modified Fe@SiO_2@PEI material modified with anhydride were fabricated for decontamination of Cr(VI) and Cd(II) in dynamic columns. The loading optimal proportion was determined using a composite of SDBS-modified maifanite and anhydride-modified Fe@SiO_2@PEI in different proportions in a column experiment. The feasibility and efficacy of the modified adsorbent were explored in column experiment with different Cr(VI) and Cd(II) concentrations and flow rates of the influent water. Yoon-Nelson model was employed to describe the column adsorption performance. This model is proved to be suitable for predicting the removal effect of heavy metals with the adsorbent. A PRB simulation test of adsorbent based on SDBS-modified maifanite and anhydride-modified Fe@SiO_2@PEI was performed in an attempt to verify the barrier property of the PRB for Cr(VI) and Cd(II). PRB was proved to be a potential material for the remediation of heavy metals in groundwater.

2. Materials and Methods

2.1. Materials. The Cr(VI)/Cd(II)-contaminated groundwater used in the research was prepared with 2.2829 g potassium dichromate and 2.1032 g cadmium nitrate as the corresponding complex heavy metal ion solution (the hexavalent chromium and cadmium reserve solution). The solution concentration is 1000 mg/L. And the simulated contaminated groundwater (influent) was obtained by diluting the reserve solution with ultrapure water.

The ferrous sulfate septihydrate (AR) used in this study was purchased from Shengao Chemical Reagent Co. Ltd in Tianjin city, China. The tetraethoxysilane (AR) was obtained from Chemical Plant in Beijing, China. The polyethyleneimine (AR) was obtained from Chemical Reagent Co., Ltd, in Shanghai city, China. The maifanite (mesh size: 60-100) provided by Zhili Environmental Protection Material Co., Ltd, was added in this research after washing with running water and drying naturally. And the main components are SiO_2 and Al_2O_3. All other chemicals and reagents were of analytical grade and used as received.

2.2. Preparation of the Adsorbent

2.2.1. Preparation of SDBS-Modified Maifanite. Modified maifanite was prepared following the procedure [21], and the detailed synthesis of modified maifanite was as follows: 1 g SDBS was taken into 200 mL deionized water. And the solution was stirred and heated to 60°C to dissolve it. Then, 10 g of the stone was added to the prepared SDBS solution while stirring, and the reaction was carried out at 60°C for 4 h by constant temperature magnetic stirring. After aging the above samples for 24 h, the aqueous phase was separated by vacuum pump, the soil samples were cleaned with deionized water for 3 times, dried, and grounded to powder at 60°C. After passing a 60-mesh sieve, the samples were obtained.

2.2.2. Preparation of Anhydride-Modified Fe@SiO_2@PEI. ZVI was prepared following the procedure [22]. Based on the synthesized ZVI, Fe@SiO_2 was prepared by Sol-Gel method [23]. ZVI (1 g) was taken and ultrasound-treated in 0.1% HCl for 10 min to remove the oxide film that may exist on the surface. Then, 1 g iron powder, 20 mL ultrapure water, 80 mL anhydrous ethanol, and 1 mL ammonia water were added into the three-neck flask. After mechanical stirring, nitrogen was added and mixed evenly. Again, 10 mL tetraethoxysilane solution (the concentration of TEOS/ethanol = 0.03 mL/1 mL) was added into the three-neck flask at a speed of 2 drops/second under the condition of stirring reaction at room temperature for 6 h. The sample is then sampled and dried in a vacuum at 60°C.

Fe@SiO_2@PEI was prepared based on the preparation of Fe@SiO_2 and was prepared as the following procedure. 0.2 g of ZVI coated by SiO_2, 50 mL xylene as the solvent, and 0.1 mL 3-triethoxysilane were taken into 100 mL polytetrafluoroethylene lining and reacted in high-pressure reaction kettle at 120°C for 24 h. Then, it was naturally cooled to room temperature, the inner wall was cleaned with ethanol, and the sample was vacuum dried (60°C). The sample was transferred to a new reactor, 10 mL 10% branched PEI was added, and the reaction continued for 24 h at 120°C. After the samples were cooled to room temperature, the samples were cleaned with ultrapure water and anhydrous ethanol and dried in vacuum (60°C) for later use.

Anhydride-modified Fe@SiO_2@PEI was prepared based on the preparation of Fe@SiO_2@PEI and was prepared as the following methods. ZVI particles grafted at 0.1 g were placed in a three-mouth flask with N-methylpyrrolidone as the solvent (100 mL) and 0.10 g of 1, 4, 5, 8-naphthotetramethyl anhydride (NTCDA) was added. After cooling to room temperature, the samples were separated by magnetic separation, cleaned with ultrapure water and anhydrous ethanol for three times, respectively, and dried in vacuum.

2.3. Proportion Selection of SDBS-Modified Maifanite and Anhydride-Modified Fe@SiO_2@PEI. The heavy metal removal studies were primarily carried out in columns packed with a mixture of silica sand and reaction materials, each containing different doses of SDBS-modified maifanite and anhydride-modified Fe@SiO_2@PEI. The mass ratios of SDBS-modified maifanite and anhydride-modified Fe@SiO_2@PEI were 9 : 1, 7 : 1, 5 : 1, 3 : 1, and 1 : 1. The loading height was the same at 90 cm. Heavy metal solution with Cr(VI) and Cd(II) concentration of 60 mg/L, respectively; a water temperature of 15 ± 3.0°C; and $pH = 6.5 \pm 0.3$ were continuously fed into the column at a rate of 10.9 mL/min by a peristaltic pump. This procedure lasted for 5 d. The reasons why we selected the above conditions are as follows. In order to explore the removal effect of heavy metals by PRB under simulated real groundwater conditions, the influent

temperature was set close to the real groundwater temperature, and the temperature of groundwater is almost at 15-17°C all year round [24, 25]. Thus, in our study, the temperature of heavy metal-polluted solution was kept in the range of 15 ± 3.0°C. Considering the application scenario of materials in this experiment and the actual groundwater conditions of the heavy metal-contaminated site in Henan province, the groundwater is not a strongly acidic or alkaline environment, the pH range is between 6.0 and 7.0 [4], and the actual groundwater flow rate of the site is about 10.90 mL/min [26, 27]. Thus, we set the initial pH values of groundwater solutions and the flow rate as 6.5 ± 0.3 and 10.90 mL/min, respectively, in this study.

The Cr(VI), total Cr (TCr), and Cd(II) concentrations of the effluent were determined. The removal efficiency of duplicates was calculated. The permeability coefficient and effective porosity were measured before and after the reaction. The loading ratio of the two adsorbents was determined.

2.4. Column Adsorption Experiments. The heavy metal removal device used in the column experiments was a self-designed plexiglass cylinder. As shown in Figure 1, the column used was 110 cm long with a 10 cm internal diameter, an 11 cm outer diameter, and a 0.5 cm wall thickness. Seven sampling holes were established: one 25 cm from the bottom of the column and six along the glass column at 15 cm intervals. One water outlet was established 105 cm from the bottom of the column. A ring with a width of 1 cm was added to the inner wall of the reactor every 30 cm to avoid marginal effects. The heavy metal removal studies were primarily carried out in columns packed with a mixture of silica sand and reaction materials, except in the column experiments with specially designed packing. Before the reaction, clean quartz sand particles (with a diameter of 1-1.5 mm) with a thickness of 10 cm were filled into the columns. After loading the reaction material, quartz sand with a thickness of 5 cm was added. The total length of the reaction column was approximately 90 cm, with a stabilizing device of 40 × 40 × 5 cm at the bottom. Heavy metal solution was continuously fed into the column at a certain rate by a peristaltic pump. The water was pumped into the reactor from the bottom to the top, where it interacted with the packing, a mixture of silica sand and reaction materials.

2.4.1. Effect of Initial Concentration on the Effluent Concentration. After loading the above determined optimal proportion of SDBS-modified maifanite and anhydride-modified Fe@SiO_2@PEI to the column, the inlet flow rate was set to 10.9 mL/min, and the concentrations of the heavy metal solution were set to 30, 60, and 90 mg/L. Then, the reactor was operated for 15 d. The heavy metal solution was regularly sampled for the determination of Cr(VI), TCr, and Cd(II) at each sampling hole. The permeability coefficient and effective porosity of the material were determined after the test.

2.4.2. Effect of Influent Velocity on the Effluent Concentration. Heavy metal solution with Cr(VI) and Cd(II) concentration of 60 mg/L, respectively, was continuously fed into three columns at rates of 5.45, 10.9, and 16.35 mL/min by a peristaltic pump for 15 d. Regular sampling was performed to determine the concentrations of Cr(VI), TCr, and Cd(II) at each sampling hole and drainage point and to determine the permeability coefficient and effective porosity of the test materials after completion.

2.4.3. Determination of Permeability and Effective Porosity. The permeability coefficients of the fillers before and after the reaction were determined by a constant head test. The device is shown in Figure 2: two pipettes were connected to the first and fifth sampling holes of the original plexiglass column, and tap water was fed from the bottom to the top at a constant flow rate. At this time, the two pressure measuring tubes exhibited a difference in liquid level. The time when the head difference and the outlet velocity were stable was recorded. The water outlet volume (V) was measured after a period of time (t). Then, the permeability was calculated by the following equation:

$$K = \frac{V\Delta L}{\Delta H A t}. \quad (1)$$

In this formula, V (expressed in cm^3) stands for the volume of water flowing out of the outlet in time t, ΔL (60 cm) represents the difference in height between the two pressure pipes, ΔH (expressed in cm) stands for the level difference between the two pressure measuring tubes, A (78.5 cm^2) represents the cross-sectional area of the plexiglass column, and t (expressed in s) stands for the test time after the pressure gauge level difference stabilizes.

The effective porosity measurement method was as follows: after the end of the dynamic column experiment, the direction of the peristaltic pump was reversed to extract as much of the remaining water in the plexiglass column as possible. The volume of the amount of water taken out is V, and the effective porosity is calculated by the following equation:

$$\eta = \frac{V}{V_0}, \quad (2)$$

where V is the volume of water pumped and V_0 is the volume of the glass column at the height of the packing.

2.4.4. Modeling of Column Data. The Yoon-Nelson model is widely used in predicting column removal efficiency based on the assumption that the decrease of the adsorption probability of each kind of adsorbate being adsorbed is proportional to the probability of adsorption and desorption on the adsorbent [23, 24]. And this model is usually used between effluent concentration and time of the column under some conditions. The Yoon-Nelson model is not only more complex than other models but does not also require detailed data on the relevant adsorbate properties, the adsorbent types, and the physical properties of the columns [25]. The form of Yoon-Nelson model can be expressed as follows

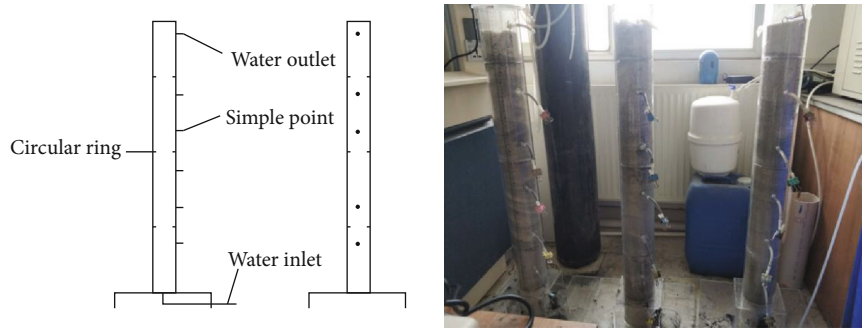

Figure 1: Schematic diagram and setup diagram of dynamic column experimental apparatus.

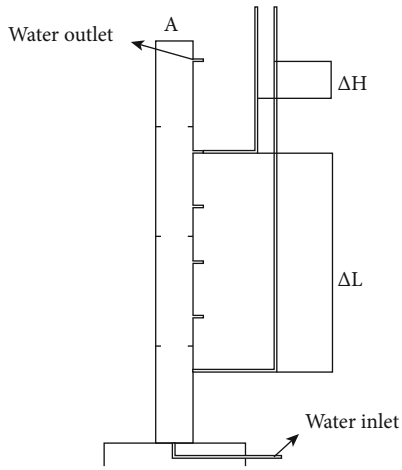

Figure 2: Schematic diagram of permeability coefficient measuring device.

[24]:

$$\frac{C_t}{C_0} = \frac{1}{1 + \exp\left[K_{YN}(T - t)\right]}. \quad (3)$$

The linearized form of the Yoon-Nelson model is as follows:

$$\ln \frac{C_t}{C_0 - C_t} = K_{YN}t - K_{YN}T, \quad (4)$$

where C_t is the concentration of heavy metal in the effluent at time t (mg/L); C_0 is the initial concentration (mg/L); K_{YN} is the constant of Yoon-Nelson (h^{-1}), which depends on the diffusion characteristics of mass transfer; and T is the time required for 50% adsorbent breakthrough (h). The coefficient K_{YN} and T can be determined from the slope and intercepts obtained from a plot $\ln [C_t/(C_0 - C_t)]$ versus t at a given condition.

2.5. Simulated PRB Test. The simulated PRB test device was made of plexiglass. The internal stages of the reaction tank (Figure 3) from left to right were the inlet area (50 mm), the reaction area (600 mm), and the outlet area (20 mm). The water level adjustment point was located in the inlet area. The reaction area was divided into a coarse sand area (50 mm), fine sand area (50 mm), reaction area (400 mm), fine sand area (50 mm), and coarse sand area (50 mm). There were four water outlets on average in the water outlet area on the glass panel. The upper water outlet was less than 5 mm from the liquid level. The device had a volume of 60 L. The cross section was a rectangle of 300 × 400 mm, the reactor had a height of 500 mm, and the loading material height was 100 mm below the top. Each area was separated by a porous plexiglass partition (400 holes) and a gauze screen. The reaction zone was filled with a composite packing with a thickness of 400 mm. A 50 mm thick coarse sand layer was placed at both ends of the reaction filler. The coarse sand (particle size is 1-2 mm) performed filtering, buffering, and protection, while the fine sand (particle size is 0.5-1 mm) acted as the simulated aquifer.

There were three reaction tanks, and each reaction tank was packed in the sequence of coarse sand, fine sand, composite filler, fine sand, and coarse sand. The quartz sand distributed water evenly and prevented scouring of the filler. Each tank was charged with nitrogen for 10 minutes and covered with glass, and the joint was smeared with Vaseline. Heavy metal solution with Cr(VI) and Cd(II) concentration of 5.0 ± 0.5 mg/L, respectively, a water temperature of 15 ± 3.0°C, and pH = 6.2 ± 0.3 were continuously fed into the reaction tank from left to right at a rate of 5.45 mL/min by a peristaltic pump for 60 d. Every night at approximately 6:00 pm, samples were withdrawn from the water outlet points in the upper part of the three columns for measurements of Cr(VI), TCr, Cd(II), dissolved iron, and pH. The results are shown as the mean plus or minus the standard deviation.

2.6. Analysis Methods

2.6.1. The Analysis Methods of the Adsorbent. A high-powered scanning electron microscope (SEM, Zeiss, Germany) was used to determine the size, morphology of magnetic nanoparticles, and element composition. Fourier transform infrared spectroscopy (FTIR) measurements were performed by using KBr as background over the range of 4000-400 cm^{-1}.

2.6.2. The Analysis Methods of the Metals. Each effluent sample was filtered through 0.45 μm filter membrane before all analysis, and the Cr(VI) concentration was determined at 540 nm by acidification using an ultraviolet and visible

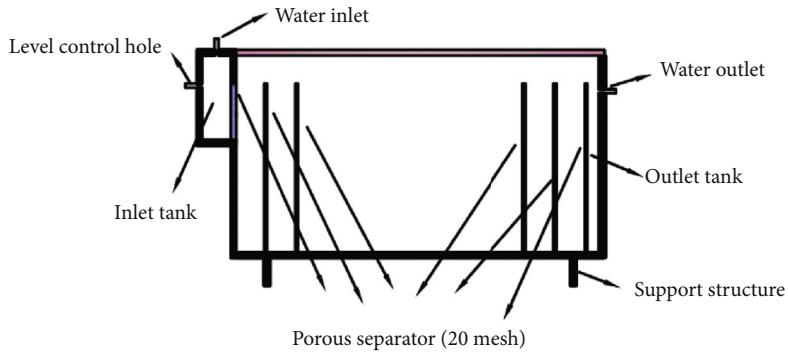

Figure 3: Schematic diagram of PRB simulated reaction tank.

spectrophotometer (UV2200, Sunny Hengping, Shanghai) (GB/T 7467-1987) according to the technical specification for groundwater environmental monitoring (HJ/T 164-2004). The concentration of TCr (357.87 nm), Cd(II) (GB/T 7475-1987) (228.80 nm), and soluble iron (GB/T 11911-89) (248.33 nm) concentrations was quantified by atomic absorption spectroscopy (AAS) (AA6880, Shimadzu, Japan) with an air flame.

3. Results and Discussion

3.1. Characterization of Modified Adsorbent and Original Adsorbent

3.1.1. SEM and EDS of Modified Adsorbent and Original Adsorbent. SEM analysis for original adsorbent and modified adsorbent was carried out to explain its surface morphological characteristics for adsorption. SEM analysis can also illustrate the porous structure and particle size of the modified adsorbent (the composite of SDBS-modified maifanite and anhydride-modified Fe@SiO_2@PEI). SEM analysis results were available as images in Figure 4. It was found that the surface of the modified adsorbent changed greatly before and after modification. As shown in Figure 4(a), the original adsorbent has a smooth surface and larger diameter. As shown in Figure 4(b), the modified adsorbent has irregular shape, broken structure, rougher surface, denser pores, and cracking and loosening in some areas. In addition, the surface of some areas is covered by a layer of substances. It may be the anionic surfactant and the maifanite surface chemically bonded or intercalated to form an organic hydrophobic layer in part of the pores of maifanite. A silicon dioxide film coating can be observed on the surface to avoid oxidation and corrosion of core iron particles in the air and can prevent iron loss during the reaction process. The surface layer of the particle is full of flaky interlayer with more holes and channels. It may be that the modifier adheres to the surface of the silicon layer, making the particle size become larger, which is also conducive to increasing the specific surface area of Fe and thus increasing the adsorption site.

It can be seen from the energy dispersion spectrum (Figure 4(d)) that C, N, and O signals are relatively high, while Cl signals are relatively weak. In addition to the fact that the coating of silica contains a large number of Si, it is also attributed to the substitution of -NH- and -COOH- groups after the condensation of PEI and naphthalenetetraformic anhydride (NTCDA) for the chlorine atoms of C-Cl bonds after the hydrolysis of silane coupling agent. The rich functional groups on the surface of PEI and NTCDA with hydrophilic properties can improve the removal ability of iron core by chelating with heavy metal ions. At the same time, the energy spectrum shows that the content of carbon and sodium increased and sulfur appeared after modification, indicating that the surfactant had been attached to the surface of the stone.

3.1.2. FIRT of Modified Adsorbent and Original Adsorbent. The functional groups are essential adsorption properties of an adsorbent. FIRT can explore the types of functional groups on the surface of modified adsorbent and characterize the adsorbent particles before and after modification in the range of 4000-500 cm^{-1}. As shown in Figure 5, in adsorbent before modification, the peaks observed at 3620.71 cm^{-1} can be assigned to stretching vibration of the -OH group of physically adsorbed water or crystallized water. The Si-O antisymmetric stretching vibration band at 1075.52 cm^{-1} indicates that the hydroxyl containing SiO_2 generated after tetraethyl orthosilicate (TEOS) hydrolysis adhered to the surface of iron core [26]. The peaks observed at 1034.38 cm^{-1} can be assigned to stretching vibration of the Si-O group. In the modified adsorbent, in addition to the original characteristic peak, many other characteristic peaks were also found which indicated that the modified adsorbent had more functional groups than the original sample. As shown in Figure 5, the absorption peak of 3432.37 cm^{-1} is due to the overlap of N-H and O-H stretching vibration, which may be caused by the introduction of a large number of amino groups in polyethylene imine. The existence of hydrogen bond reduces frequency and broadens spectrum peak. The peak at 454.31 cm^{-1} and 453.81 cm^{-1} is due to the symmetric stretching vibration of Si-O, and the peak at 770.69 cm^{-1} is due to the bending vibration of Si-O. The vibration band of C=O at 1666.00 cm^{-1} [27] indicates that carbonyl compound anhydride has been introduced. The absorption band between 1660 and 1455.87 cm^{-1} is the overlapping peak formed by the stretching vibration of C-N and C=C and the bending vibration of C-H. The absorption peak of organic sulfonate was found. The absorption band between 2920.09 cm^{-1} and 2850.80 cm^{-1} indicates the existence of methyl (-CH_2-) and methylene (-CH_3) of sodium

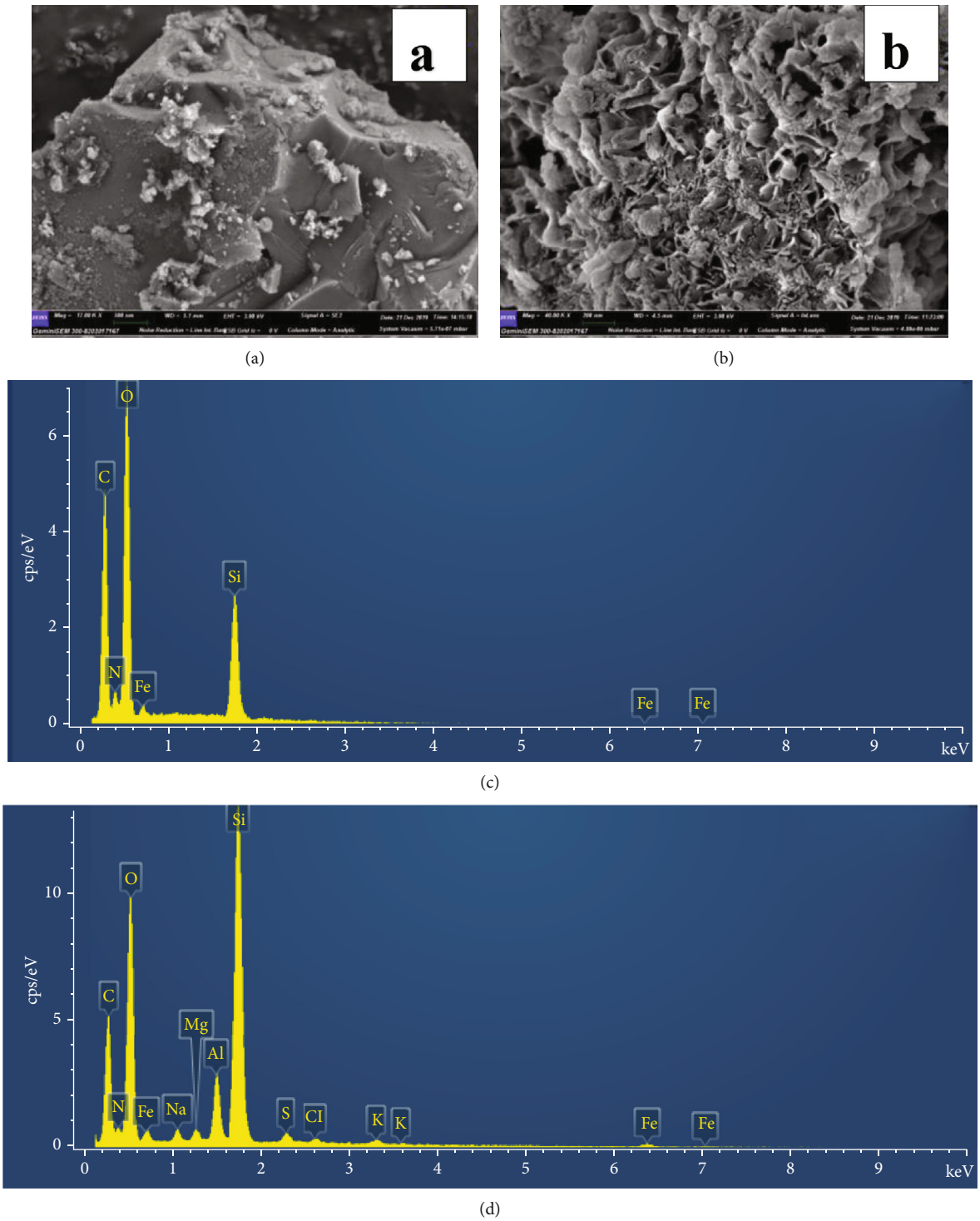

Figure 4: SEM of original adsorbent (a) and modified adsorbent (b) and EDS spectra of the adsorbent before (the composite of ZVI and maifanite) (c) and after (the composite of Fe@SiO_2@PEI and modified maifanite) (d) modification.

dodecylbenzenesulfonate groups. The peaks observed at 1170.52 cm^{-1} can be assigned to stretching vibration of the sulfonic S=O group in the benzene ring. The additional peak beyond 1000 cm^{-1} can be assigned to fingerprint regions of functional groups of metal oxides. This indicates that the organic sulfonate enters the layers of maifanite and forms a strong force with the laminate [28].

3.2. Continuous Column Experiments

3.2.1. Proportion Selection of SDBS-Modified Maifanite and Anhydride-Modified Fe@SiO_2@PEI. The key to the success of PRB is to choose suitable materials as filler, and the proportion of SDBS-modified maifanite and anhydride-modified Fe@SiO_2@PEI materials is very important. As can

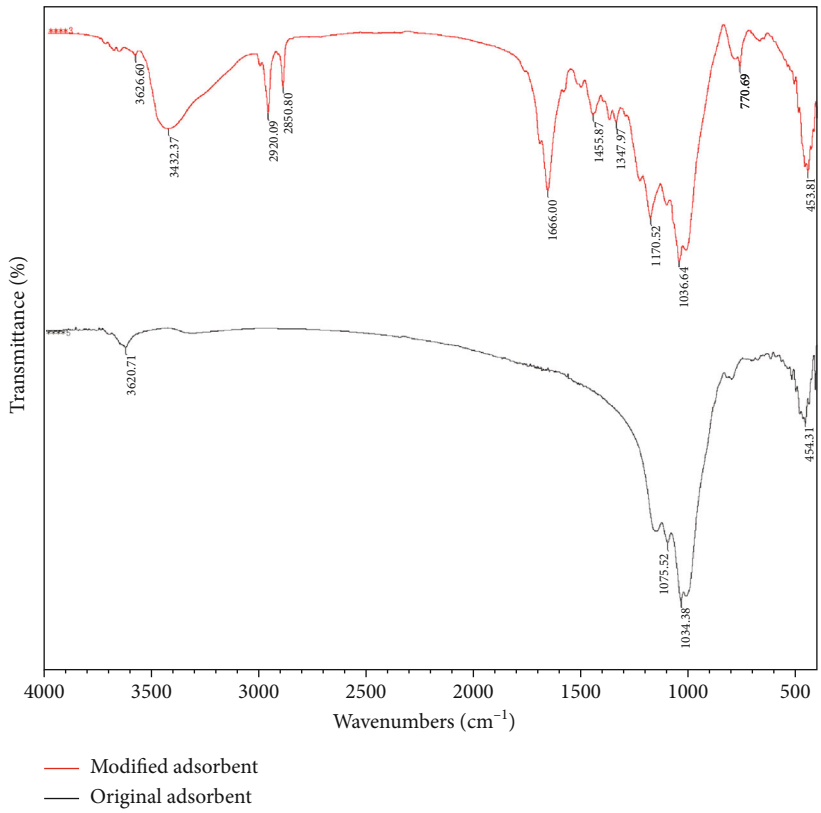

Figure 5: FIRT of original adsorbent (the composite of Fe@SiO_2 and maifanite) and modified adsorbent (the composite of Fe@SiO_2@PEI and modified maifanite).

be seen from Figure 6(a), with the increase of the proportion of anhydride-modified Fe@SiO_2@PEI, the removal rate of heavy metals (Cr(VI), TCr, and Cd(II)) in the effluent increased. Therefore, the remediation effect can be improved by increasing the proportion of anhydride-modified Fe@SiO_2@PEI. However, the reaction mechanism is mainly that heavy metal ions form coprecipitation and attach to the surface of the material, and the particle size of anhydride-modified Fe@SiO_2@PEI is too small (0.106-0.150 mm), which leads to defects if anhydride-modified Fe@SiO_2@PEI is used as single filler or the proportion of anhydride-modified Fe@SiO_2@PEI is too high [29]. It was found that the increase of the proportion of anhydride-modified Fe@SiO_2@PEI led to a significant decrease in the permeability coefficient and the internal agglomeration phenomenon became more serious for 5 d in Figure 6(b). The permeability coefficient has been reduced to 0.019 cm/s after reaction when the ratio of SDBS-modified maifanite and anhydride-modified Fe@SiO_2@PEI was 1 : 1. It is no longer able to meet the requirement that the permeability coefficient of PRB material is at least 1.5-2.5 times higher than the permeability coefficient of the local soil [30], which is easy to cause the internal blockage of PRB, make the underground water level rise or flow around, and lose the remediation effect. Furthermore, considering that the cost of anhydride-modified Fe@SiO_2@PEI was much higher than that of SDBS-modified maifanite, the proportion of SDBS-modified maifanite should be increased, so the composite material with a mass ratio of 5 : 1 was used as the filler for subsequent tests.

3.2.2. Effects of Initial Cr(VI) and Cd(II) Concentrations. The breakthrough curves obtained by changing initial Cr(VI) and Cd(II) concentrations from 30 to 60 mg/L at a flow rate of 10.9 mL/min are given in Figures 7 and 8. The breakthrough curve for columns was determined by plotting the ratio of C_t/C_0 (C_t and C_0 are the Cr(VI) and Cd(II) concentrations of effluent and influent, respectively) against time, as shown in Figures 7 and 8. As expected, an increased inlet concentration gave an earlier breakthrough curve and the Cr(VI) and Cd(II) adsorption capacities were greatest at the greatest concentration; in turn, the Cr(VI) and Cd(II) removal rates ($1 - C_t/C_0$) were the lowest. The findings could be attributed to the fact that the higher concentration gradient increased the mass transfer coefficient or the diffusion coefficient leading to a faster transport [31]. As we all know, adsorption kinetics is related to free binding sites and the concentration of heavy metals. Therefore, it is expected that the capacity of the given substrate for Cr(VI) and Cd(II) uptake dramatically increased with the increase of the inlet heavy metal concentrations due to the saturation of available free sites. The maximum removal rates of Cr(VI) were 99.93%, 99.71%, and 99.61% at 6 h, respectively, at an initial Cr(VI) concentration of 30, 60, and 90 mg/L. And

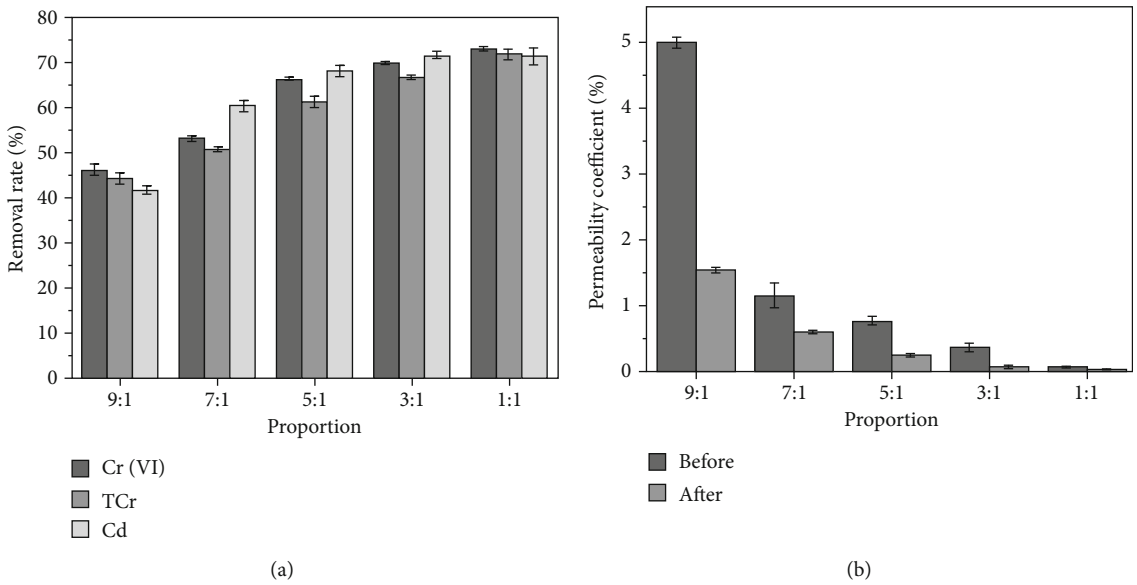

FIGURE 6: Effect of the proportion of SDBS-modified maifanite and anhydride-modified Fe@SiO_2@PEI on heavy metal removal rate (a) and permeability coefficient (b).

the highest removal efficiency of Cd(II) was 99.79%, 99.71%, and 98.64% at 6 h, respectively, at an initial Cd(II) concentration of 30, 60, and 90 mg/L.

Moreover, it was found that higher initial concentrations decreased the exhausted time in spite of delaying the increase of C_t/C_0. The probable reason is the reaction sites becoming more quickly saturated with increasing inlet Cr(VI) and Cd(II) concentration in the adsorption column. Saturation occurred after 360 h at 30 mg/L Cr(VI) inlet concentration while as the exhausted time appeared after 312 and 264 h at the inlet Cr(VI) concentration of 60 and 90 mg/L, respectively. The exhausted time was 216 and 264 h at the inlet Cd(II) concentration of 60 and 90 mg/L, but the equilibrium did not occur at the inlet concentration of 30 mg/L during the entire experiment. Interestingly, the higher the inlet concentration is, the bigger the ratio of C_t/C_0 is before 60 h; however, the lower the inlet concentration is, the smaller the value of C_t/C_0 is after 60 h (Figure 7), which is more noticeable in Figure 7(a) (sampling hole 1) and almost insignificant in Figures 7(b)–7(f).

Similarly, the trends are found in Figure 8. This phenomenon has never been found in previous researches. Therefore, I suppose that heavy metal inlet leads to a decrease in microbial activity, which has an effect on the uptake of heavy metals in the columns in consequence (the microorganism is a parameter that affects the heavy metal's capture ability). The trend became slight from sampling holes 1-6 shown in Figures 7 and 8, respectively. This observation may be due to the fact that the heavy metal concentrations gradually decreased along the column resulting in the activity of microorganism decreased along the column. This phenomenon is worth to explore further.

3.2.3. Effect of Flow Rate. Effects of different flow rates (5.45, 10.9, and 16.35 mL/min) on adsorption performance were operated in the column experiments at the initial Cr(VI)/Cd(II) concentration of 60 mg/L (Figures 7 and 8). The C_t/C_0 values of Cr(VI) at each sampling hole increased at each flow rate until the C_t/C_0 values reached stability during the entire column experiment. The initial adsorption reaction of Cr(VI) was very rapid, which may be attributed to more available adsorption for capturing Cr(VI) in the solution [32]. The following stable C_t/C_0 values were possibly due to the gradual occupancy of these binding sites. Furthermore, it was noticed that a higher flow speed led to the lower removal rate of Cr(VI) in the collected effluent sample before reaching saturated adsorption. Similarly, the removal rate of Cd(II) decreased from 75.50% to 39.76% with an increase in flow rate from 1 to 16.35 mL/min at 48 h (Figure 9(a)). Predictably, higher flow rates were not conducive to the removal of contaminants from aqueous solutions [33, 34].

In addition, the breakthrough curve becomes steeper and earlier exhaustion times were observed when the flow rate was increased from 1 to 16.35 mL/min. It is probably due to higher flow rate that induced shorter residence time in the adsorbing column, resulting in the inadequate reaction proceeded [35]. For Cr(VI) adsorption, the exhausted times at sampling hole 1 were 312, 288, and 240 h at the flow rates of 5.45, 10.9, and 16.35 mL/min, respectively (Figure 10(a)). Meanwhile, the exhausted time at sampling holes 2, 3, 4, 5, and 6 increased from 240 to 264, 264, 288, and 312 h; 216 to 240, 240, 264, and 312 h and 168 to 192, 216, 216, and 240 h, respectively, with an increase in the flow rate from 1 to 16.35 mL/min (Figures 10(b)–10(f)). For Cd(II) adsorption, the exhausted time at sampling holes 2, 3, 4, 5 and 6 increased from 240 to 264, 264, 264 and 288 h; 216 to 240, 264, 288 and 312 h and 96 to 144, 168, 192 and 216 h, respectively, with an increase in the flow rate from 1 to 16.35 mL/min (Figure 9(a)-9(f)). The results showed that

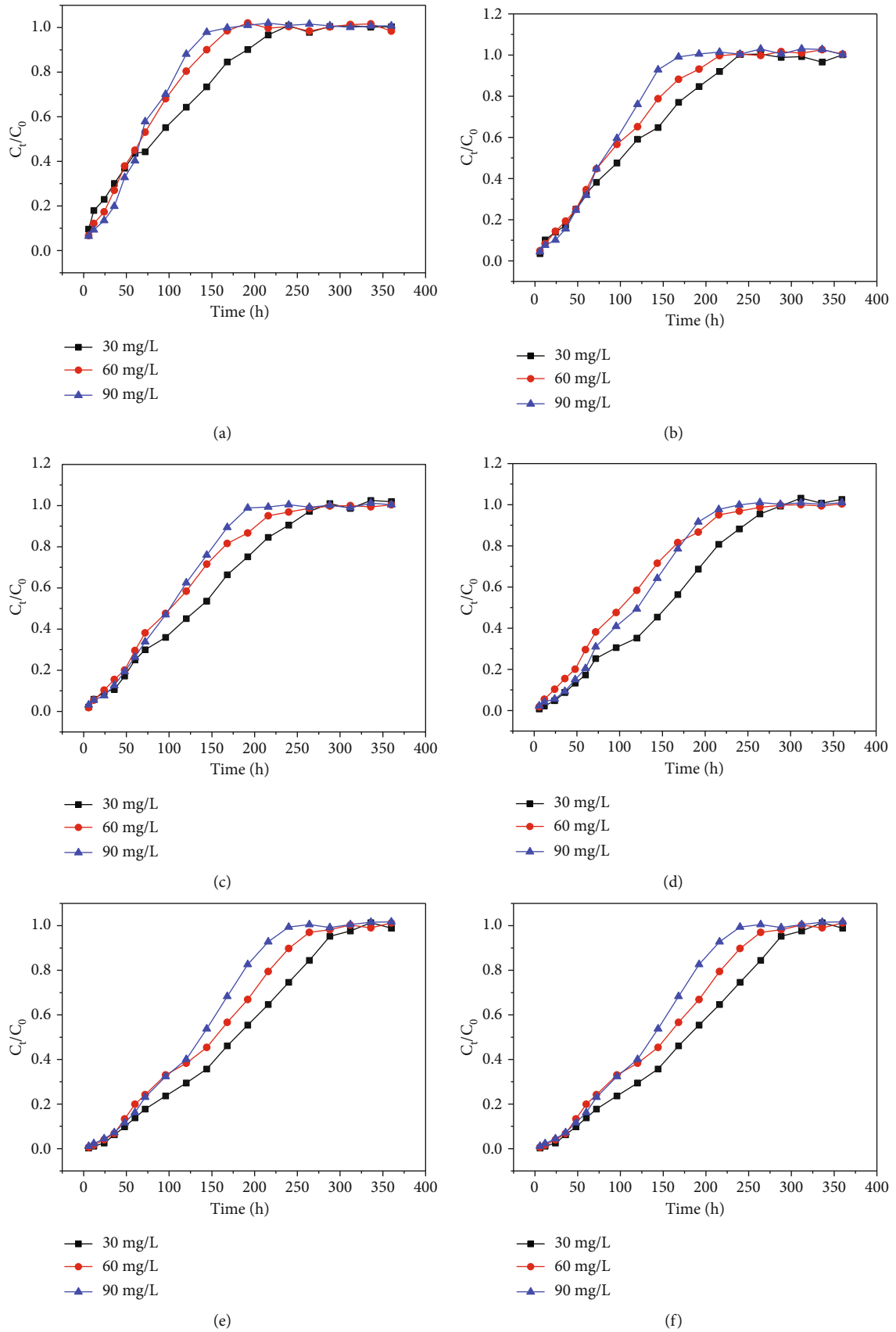

Figure 7: Effects of initial Cr(VI) concentration of each sampling hole at a flow rate of 10.9 mL/min: (a) sampling hole 1; (b) sampling hole 2; (c) sampling hole 3; (d) sampling hole 4; (e) sampling hole 5; (f) outlet hole.

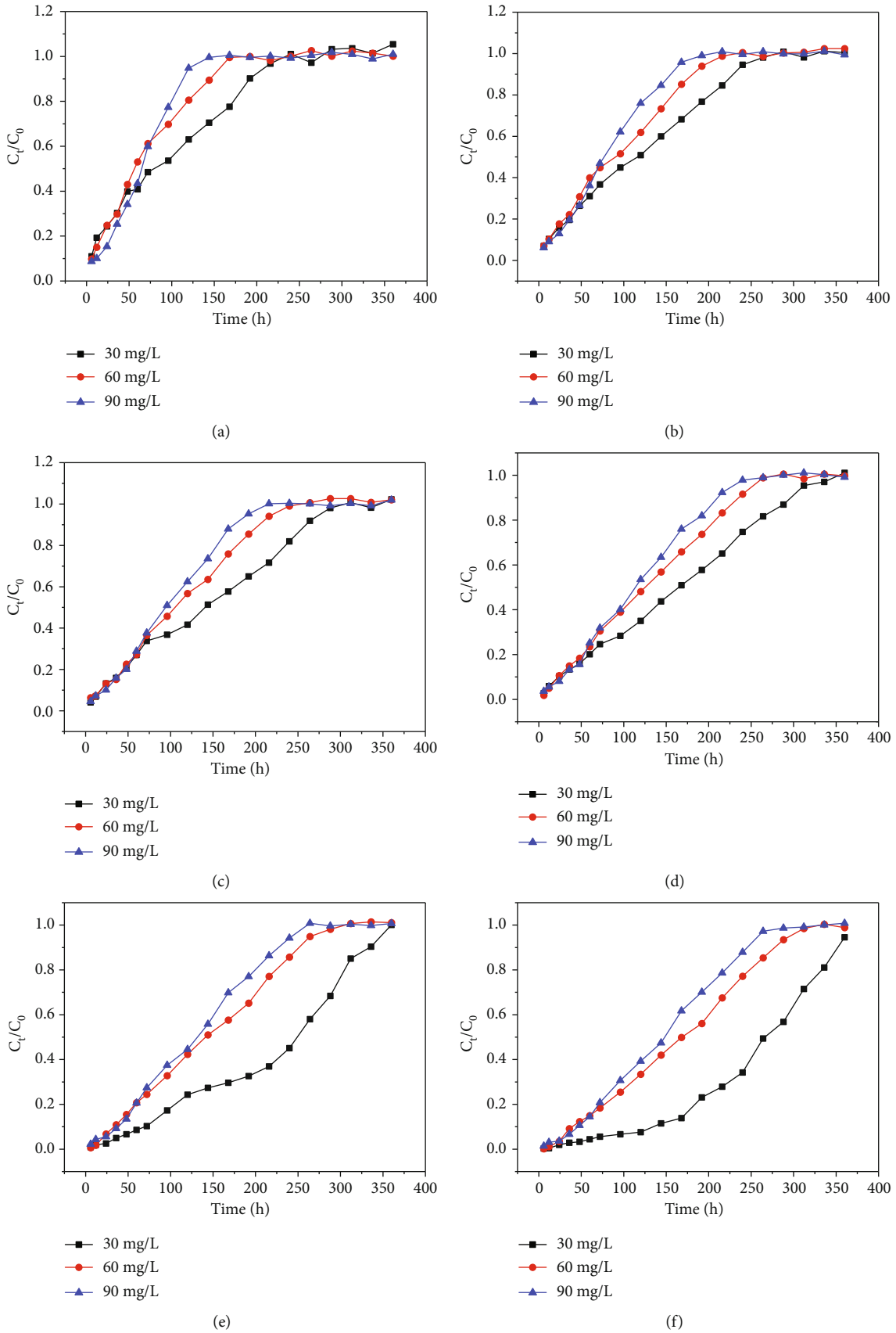

Figure 8: Effects of initial Cd(II) concentration of each sampling hole at a flow rate of 10.9 mL/min: (a) sampling hole 1; (b) sampling hole 2; (c) sampling hole 3; (d) sampling hole 4; (e) sampling hole 5; (f) outlet hole.

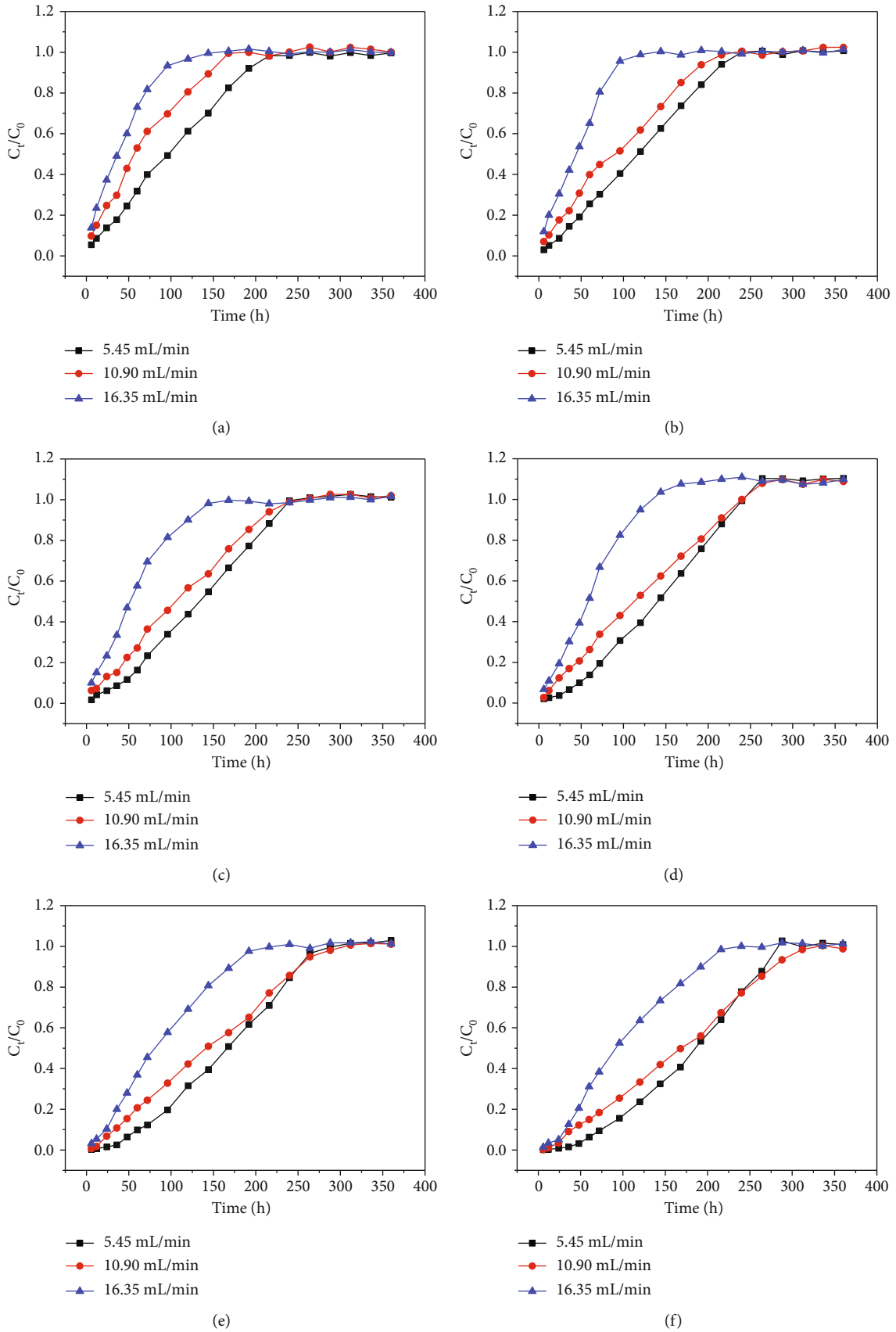

Figure 9: Effects of initial flow rate on Cd(II) of each sampling hole at an initial Cd(II) concentration of 60 mg/L: (a) sampling hole 1; (b) sampling hole 2; (c) sampling hole 3; (d) sampling hole 4; (e) sampling hole 5; (f) outlet hole.

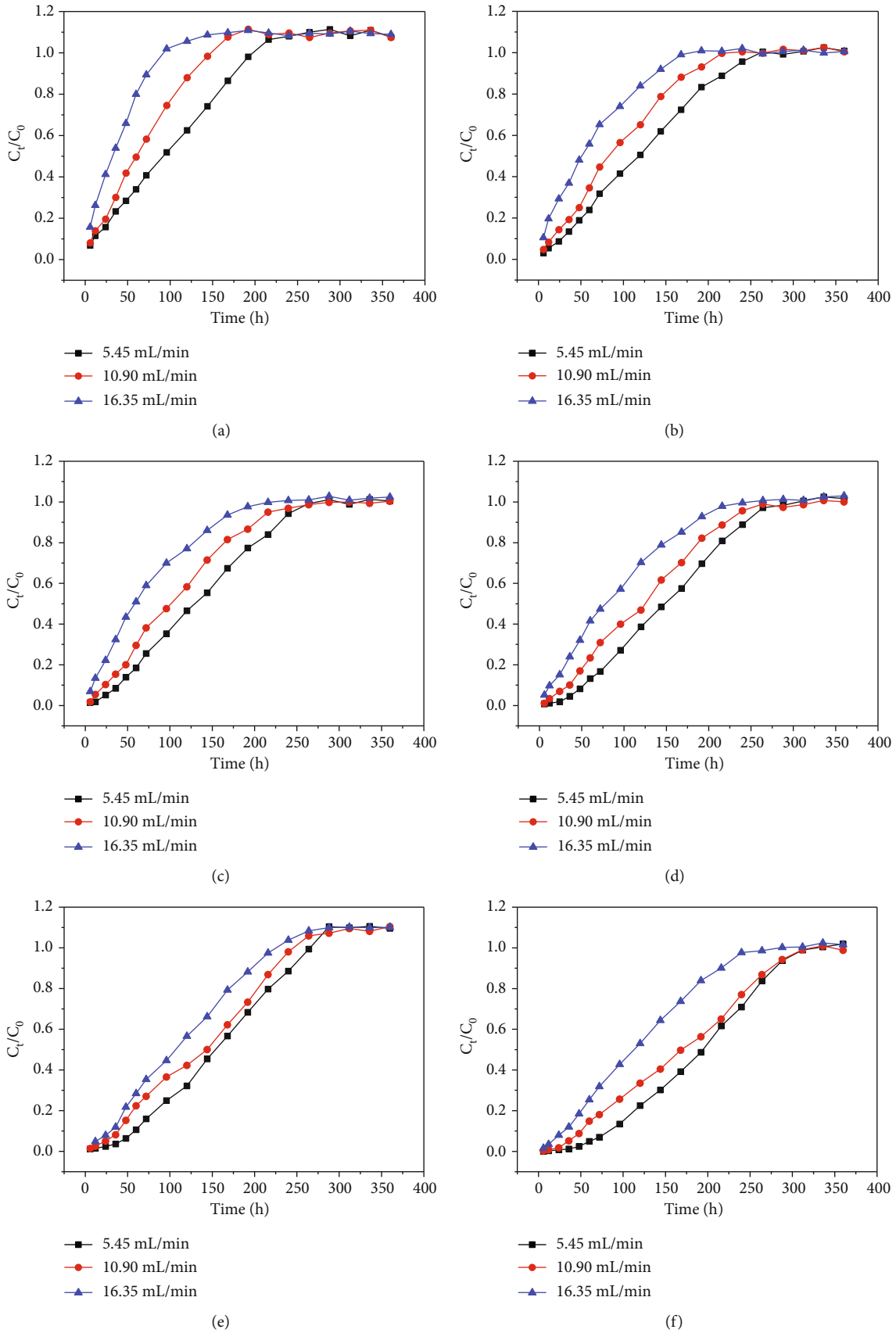

Figure 10: Effects of initial flow rate on Cr(VI) of each sampling hole at an initial Cr(VI) concentration of 60 mg/L: (a) sampling hole 1; (b) sampling hole 2; (c) sampling hole 3; (d) sampling hole 4; (e) sampling hole 5; (f) outlet hole.

as the Cr(VI) and Cd(II) passed from sampling holes 1-6, the exhausted time along the column continuously increased during the whole operation. The increase may be explained by the long distance between the sampling holes 1 and 6 leading to the retention of some Cr(VI) and Cd(II) inside the bottom half of the filling. Another probability may be interception of some heavy metal ions due to redox reaction or coprecipitation, resulting in the lower Cr(VI) and Cd(II) concentrations at sampling hole 6 relative to those at sampling holes 1-5. Therefore, there was a small amount of Cr(VI) and Cd(II) in the collected effluent.

The flow rate reflects the hydraulic load to some extent, and the groundwater velocity in the contaminated sites is an important hydrogeological condition in practical application. Thus, the PRB thickness can be determined according to the actual flow rate. If the penetration time is too short, the length of the reaction medium can be increased, such as increasing the PRB thickness or adopting the form of series connection to meet the expected effect. For example, with the sampling hole 1 upward to the outlet hole, and the residence time of the target pollutants in the fillers, dosage of adsorbent and the penetration time increase with the increase of the filler height.

3.2.4. Changes in Permeability Coefficient and Porosity after Column Experiment. The permeability coefficient and effective porosity of the fillers in five groups of dynamic columns were tested (Figure 11). Porosity, which represents the degree of compaction and the permeability coefficient, can represent the space blockage inside the packing and the resistance to water flow. Compared with the original fillers, the content of particles on the surface of the reacted fillers increased due to the formation of precipitation, and the permeability coefficient and porosity of the reacted fillers decreased to different degrees [36]. This phenomenon may also be due to the fact that small particulate matter moved into the pores of the fillers, resulting in a decrease in permeability under the scour of water flow.

3.2.5. Simulation of Breakthrough Curves. As shown in Table 1, the Yoon-Nelson model adequately reproduced the experimental results for the columns (the heavy metal removal performance), and the obtained R^2 values were more than 0.9. Based on the R^2 (more than 0.9) values, the Yoon-Nelson model is considered suitable to describe the Cr(VI) and Cd(II) column adsorption [37, 38].

The experimental results have been fitted to the Yoon-Nelson model through nonlinear regression. The time (T) required for 50% Cr(VI) and Cd(II) breakthrough under different initial concentrations and flow rates can be seen in Table 1. The time required for 50% adsorbent breakthrough T decreased from 209.59 to 154.44 h for Cr(VI) and 257.29 to 147.54 h for Cd(II), respectively, with increasing initial concentrations. On the other hand, with the increase in flow rate, T values of Cr(VI) and Cd(II) decreased from 191.59 to 128.88 h and 186.06 to 123.03 h, respectively. The experimental result was in very good agreement with the above findings that the effluent Cr(VI) and Cd(II) concentrations of each sampling hole at the same time increased as the initial concentrations of heavy metals increased and flow rates decreased, but the exhausted time decreased. Additionally, the kinetics constant K_{YN} values decreased with the increasing flow rates but increased with an increase in the initial concentrations of Cr(VI) and Cd(II). The phenomenon was consistent with the result of the previous study [39]. In the previous study, when Ammonium Molybdate Phosphate-polyacrylonitrile (AMP-PAN) was used for cesium (Cs) adsorption in acidic waste solution in a fixed bed column, it was observed that the T value reduced from 258 to 148 min and the K_{YN} value increased from 4.6×10^{-2} to 5.6×10^{-2} h^{-1} with an increase in initial Cs concentration. However, the values of K_{YN} and T decreased when the quantity of flow increased.

Yoon-Nelson describes the breakthrough curve with high correlation coefficients. The heavy metal removal performance predicted by the Yoon-Nelson model exhibited a similar trend as the heavy metal removal effect in our experimental results.

3.3. Simulated PRB Test. To explore the feasibility of applying the selected materials in a PRB, the PRB simulation reactor was used for a dynamic trial. When the inflow velocity was set to 5.45 mL/min (much of the space inside the tank was filled with the fillers, so the actual flow rate was much higher than 5.45 mL/min), the inflow started to flow out from the outlet at the bottom of the tank started after 2 h according to the actual observation. Thus, the hydraulic retention time was approximately 2 h. The peristaltic pump was continuously filled with water, and the daily water treatment volume was approximately 90 L. According to the quality standard for groundwater (GB/T14848), the initial Cr(VI) and Cd(II) (coexisting in the influent) concentrations are 100 (5.0 ± 0.5 mg/L) and 500 (5.0 ± 0.5 mg/L) times higher than the standard, respectively, in order to apply to the class III water level evaluation standard of the centralized drinking water source and industrial and agricultural water.

The relationship between the concentrations of heavy metal ions in the daily effluent of the reactor and time during the pilot test was investigated (Figure 12(a)). When the cumulative water yield was 2160 L on 24 d, the Cd(II) content exceeded the standard value; meanwhile, when the cumulative water yield reached 2880 L on 33 d, the Cr(VI) content exceeded the standard limit. Combined with the relationship between the effluent Cr(VI) and TCr concentrations, it was found that there was no soluble form of Cr(III) in the influent water. It could be ascribed to the fact that Cr(VI) was adsorbed directly by SDBS-modified maifanite and anhydride-modified Fe@SiO_2@PEI or that cationic Cr(III) being reduced by ZVI was more easily adsorbed by SDBS-modified maifanite with negative charge on the surface. At the later stage of the reaction, although anhydride-modified Fe@SiO_2@PEI still had a strong reducing capacity, the adsorption sites on the adsorbent surface gradually decreased and Cr(III) was washed into the solution in the form of hydroxides, resulting in the gradual increase in the Cr(III) concentration. As mentioned above, the contents of Cr(VI) and Cd(II) exceeded the groundwater-related limits on 33 and 24 d, respectively; however, the adsorbent had

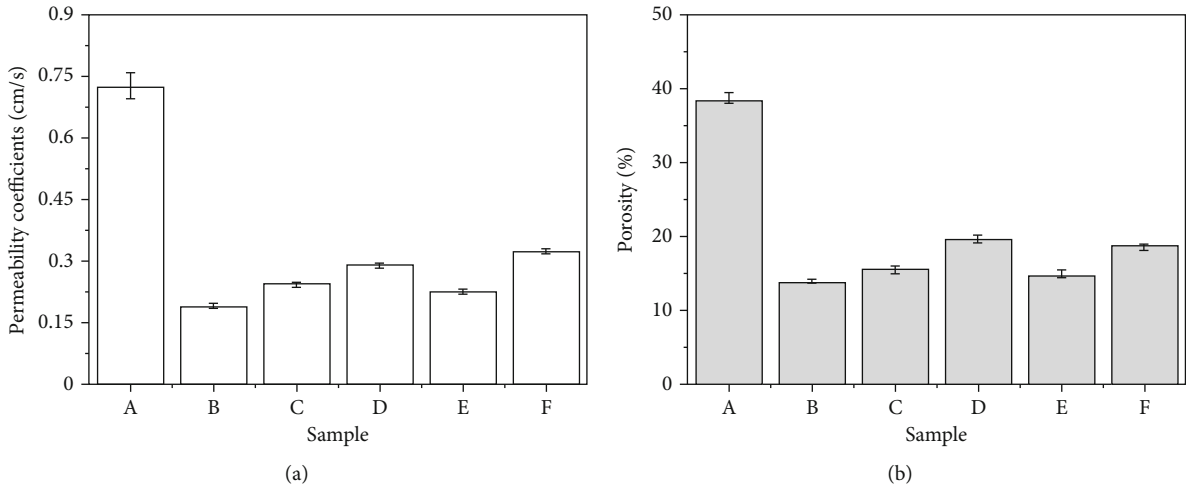

Figure 11: Changes in permeability coefficient (a) and porosity (b) of each reaction column after column experiment.

Table 1: Yoon-Nelson model fitting parameters.

Contaminant	Parameter	Concentration (mg/L)			Flow rate (mL/min)		
		30	60	90	5.45	10.90	16.35
Cr(VI)	K_{YN} (h^{-1})	0.0224	0.0243	0.0279	0.0288	0.0243	0.0232
	T (h)	209.59	175.63	154.44	191.59	175.63	128.88
	R^2	0.9713	0.9567	0.9785	0.9481	0.9366	0.9812
Cd(II)	K_{YN} (h^{-1})	0.0185	0.0242	0.0244	0.0284	0.0242	0.0229
	T (h)	257.29	165.48	147.54	186.06	147.54	123.03
	R^2	0.968	0.9567	0.9732	0.9525	0.9366	0.9425

not completely failed, and the removal rates of Cr(VI) and Cd(II) still reached 85.94% and 83.45%, respectively, indicating the strong removal ability by the end of 60 d of the test. Compared with the 5.45 mL/min flow rate set in this study, the seepage velocity of groundwater in actual sites, especially confined water, is slower, and the hydraulic retention time is longer, which are more conducive to the adsorption of Cr(VI) and Cd(II) in water by the adsorption materials.

The total soluble iron and pH in the daily effluent are shown in Figure 12(b). With the continuous progression of the reaction, the total soluble iron content in the effluent increased. According to equations (5), (6), (7), (8), (9), Cr(VI) was reduced to Cr(III) [40–42] and ZVI was oxidized to Fe(II) or Fe(III) under a series of redox reactions, leading to the increase of the total soluble iron content and pH in the solution. At the beginning of the reaction, the quantity of Cr(VI) participating in the redox reaction was low. Moreover, the resulting precipitation could also be absorbed by SDBS-modified maifanite and anhydride-modified Fe@SiO_2@PEI. At the end of the experiment, the iron had suffered a great deal of corrosion in the process of reduction of Cr(VI). Since the adsorption sites on the surfaces of SDBS-modified maifanite and anhydride-modified Fe@SiO_2@PEI were limited, the amount of Fe(II) or Fe(III) entering the water began to increase. In addition, there was a large amount of dissolved oxygen in influent without deoxidation treatment continuously brought in by the peristaltic pumps, which promoted the aerobic corrosion of iron and formed lepidocrocite (γ-FeOOH), magnetite (Fe_3O_4), and magnetohematite (γ-Fe_2O_3) [43]. It resulted in an increase in the total iron concentration in effluent. Additionally, the pH of the solution increased gradually due to the production of OH^- in water according to the Cr(VI) reduction process. However, the Fe content and pH value in effluent still met the requirements of grade III water (Fe < 0.3 mg/L and pH between 6.5 and 8.5) in the quality standard for groundwater (GB/T 14848). The concentrations of heavy metal ions did not reach their initial concentrations during the whole reaction stage, and the reaction inside the system was ongoing. Therefore, the total soluble iron concentration and pH of the effluent were on the rise.

$$CrO_4^{2-} + 3FeO + 8H^+ \longrightarrow Cr^{3+} + 3Fe^{2+} + 4H_2O \quad (5)$$

$$Cr_2O_7^{2-} + 6\,FeO + 14H^+ \longrightarrow 2Cr^{3+} + 6Fe^{2+} + 7H_2O \quad (6)$$

$$Fe + Cr_2O_7^{2-} + 7H_2O \longrightarrow 2Cr(OH)_3 + Fe(OH)_3 + 6OH^- \quad (7)$$

$$Fe + CrO_4^{2-} + 4H_2O \longrightarrow Cr(OH)_3 + Fe(OH)_3 + 2OH^- \quad (8)$$

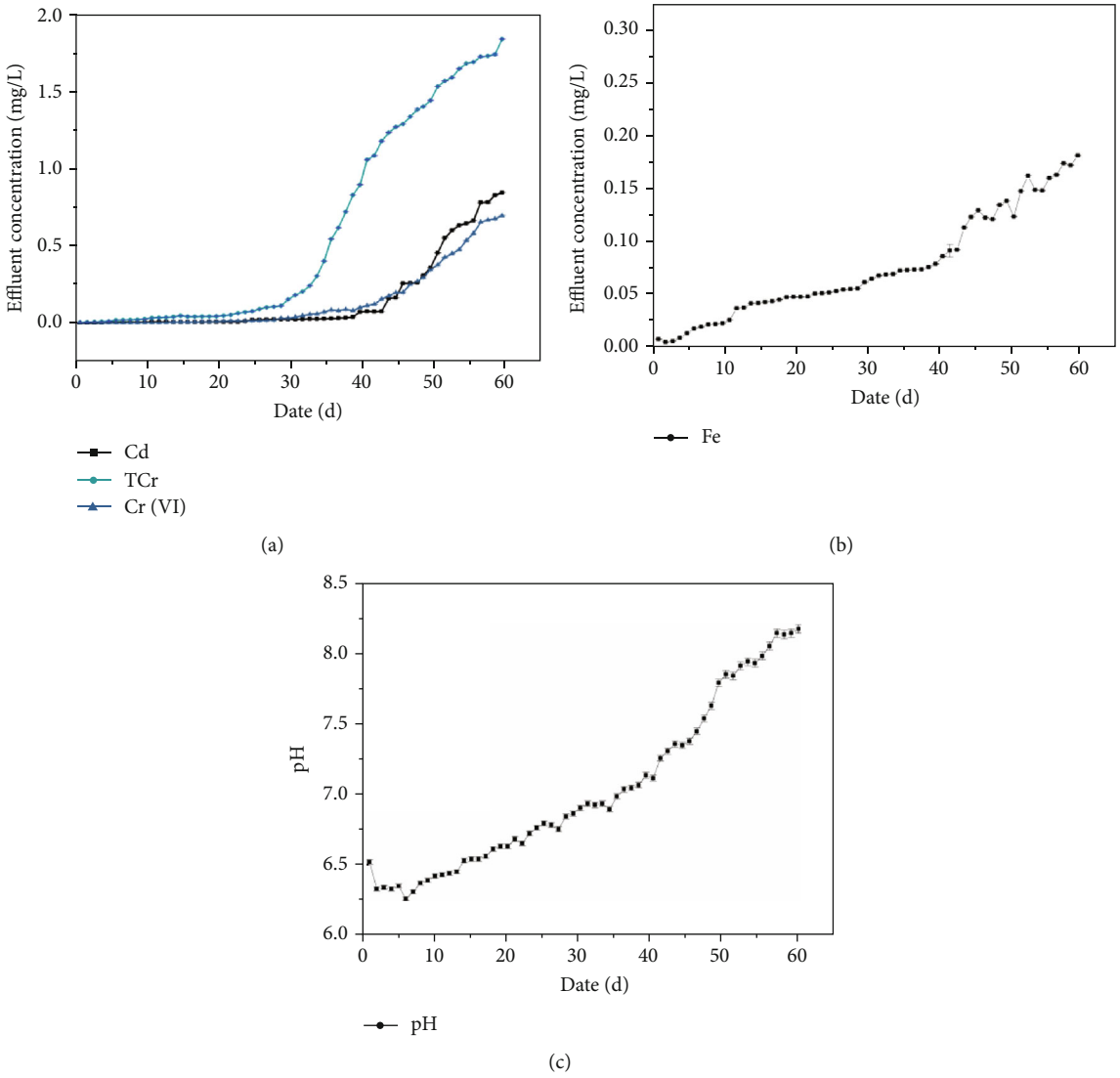

Figure 12: The changes of PRB effluent heavy metal concentration (a), soluble total iron concentration (b), and pH (c) were simulated when the influent Cr(VI) and Cd(II) (coexisting in the influent) concentrations are 5.0 ± 0.5 mg/L and 5.0 ± 0.5 mg/L.

$$CrO_4^{2-} + 3Fe^{2+} + 4H_2O \longrightarrow 3Fe^{3+} + Cr(OH)_3 + 5OH^- \quad (9)$$

Throughout the test, the daily effluent volume remained basically the same. There was no water outflow of the overflow hole in the water inlet tank. The liquid level in the tank was basically the same as the height of the filler. In other words, all the water pumped into the water tank by the peristaltic pump completely flowed through the PRB filler and flowed out through the outlet hole after the reaction. Under neutral pH conditions, the hydroxides ($Cr(OH)_3$, $Fe(OH)_3$, and $Cd(OH)_2$) formed by the three metal ions had low solubility and were easy to precipitate on the surfaces of SDBS-modified maifanite and anhydride-modified Fe@SiO_2@PEI [44, 45]. The formed precipitation was trapped in the reactor, resulting in the increase of medium resistance, which hindered fluid movement in the PRB to some extent. Therefore, the fillers may have been partially blocked, but the flow pattern was not changed.

In the practical application of PRBs, sand or gravel is usually mixed with reactive iron shavings, which are used as a mixed backfilling material in underground trenches [46]. In the present work, SDBS-modified maifanite, which also has the property of adsorbing heavy metal ions, and anhydride-modified Fe@SiO_2@PEI were used in combination. The synergistic effect between the two materials improved the removal effect of the system. Anhydride-modified Fe@SiO_2@PEI reacted with Cr(VI) and Cd(II) via processes such as coprecipitation, surface adsorption, and chelation with organic group ligands. Reduction also occurred, which made Cr(VI) change to the more stable and more soluble form Cr(III) and changed $Cr_2O_7^{2-}$ and CrO_4^{2-} in the form of oxygen-containing anions into cationic Cr^{3+}. The charge of Cr^{3+} has the same charge as Cd^{2+} and is more likely to be attracted by the electrostatic attraction of maifanite modified with an anionic surfactant.

As known from the above dynamic column experiment, the precipitation of heavy metal hydroxides will reduce the porosity and permeability of the fillers. Compared with anhydride-modified Fe@SiO_2@PEI, SDBS-modified maifanite has a larger particle size and can be used as a skeleton material to increase the internal space of the filler, reducing the disturbance to the flow state and extending the service life of the PRB. The permeability coefficient of the PRB filler (generally more than 2 times higher than the permeability of the local aquifer) [47] and the removal efficiency of pollutants are the two most important parameters. Ordinary materials rely on surface adsorption to remove contaminants. The smaller the particle size is, the larger the specific surface area is, and the better the removal effect of pollutants is. However, the smaller the particle size resulted to the higher the surface energy, causing the decrease in the effective porosity and the permeability coefficient. Therefore, the proportion of SDBS-modified maifanite and anhydride-modified Fe@SiO_2@PEI selected in this manuscript is not necessarily applicable to all sites. The hydrogeological conditions of the contaminated site, including the flow direction and burial depth of groundwater, slope, pollutant types and concentrations, permeability coefficient, and impermeable layer, must be considered to reasonably select the PRB type, processing method, filler proportions, and specific size, so as to meet the treatment requirements and reduce the project investment.

4. Conclusions

This study identified SDBS-modified maifanite and anhydride-modified Fe@SiO_2@PEI as a suitable adsorbent to be utilized for removal of Cr(VI) and Cd(II) from groundwater. SDBS-modified maifanite with a large diameter (40-60 mesh) can provide support and increase the permeability coefficient and porosity, and anhydride-modified Fe@SiO_2@PEI can convert Cr(VI) existing in the form of oxygen anions ($Cr_2O_7^{2-}$ and CrO_4^{2-}) to Cr(III) and improve the adsorption capacity of maifanite, which has a negative surface charge. The synergistic effect between these materials improved the removal effect of the system. The removal rates of Cr(VI) and Cd(II) reached 99.93% and 99.79% at an initial Cr(VI) and Cd(II) concentration of 30 mg/L with the flow rate of 10.9 mL/min, respectively, at 6 h. Column experiment of the studied metals indicated that the penetration time decreased with the increase in the initial concentration and flow rate. The heavy metal adsorbed amounts of the adsorbent depended on the initial concentration and flow rate. In the PRB simulation test, the concentrations of the heavy metal ions Cr(VI) and Cd(II) exceeded the standard values (0.05 and 0.01 g/L) at 33 and 24 d, respectively. Meanwhile, the treated water volume was 2160 and 2280 L, respectively. The soluble total iron and pH values still conformed to the requirements of grade III water in the quality standard of groundwater (GB/T14848). The Yoon-Nelson model was successfully used to predict the breakthrough curves under using different initial concentrations and flow rates and provide maximum removal efficiency of materials, which were necessary to ensure complete use of materials and save investigation and operation costs during the design of PRB. From these results, the use of SDBS-modified maifanite and anhydride-modified Fe@SiO_2@PEI as an adsorbent for Cr(VI) and Cd(II) removal is potentially cost-effective and may provide an alternative method for Cr(VI) and Cd(II) removal from contaminated groundwater.

Data Availability

All data, models, and code generated or used during the study appear in the submitted article.

Conflicts of Interest

The authors declare that they have no known competing financial interests or personal relationships that could have appeared to influence the work reported in this paper.

Authors' Contributions

Yalin Zhai was responsible for writing original draft. Zhenzhen Huang was responsible for formal analysis, writing, review, editing, and visualization. Peng Ren was responsible for supervision. Jianlei Gao was responsible for supervision. Zhijun Chen was responsible for supervision. Shunling Li was responsible for supervision. Jingqing Gao was responsible for visualization, conceptualization, methodology, writing, review, and editing.

Acknowledgments

The majority of this work was supported by the Major Special Science and Technology Project of Henan Province (181100310300), the National Science and Technology Major Project (2017ZX07602-003-002), the fellowship of China Postdoctoral Science Foundation (2020TQ0284 and 2020M682355), Zhongyuan Yingcai Jihua (ZYYCYU202012183), Henan Postdoctoral Foundation (202003027), and Key open fund project of Henan Key Laboratory for water pollution prevention and remediation (CJSP2021007).

References

[1] Z. Z. Jia, Y. H. Shu, R. L. Huang, J. G. Liu, and L. L. Liu, "Enhanced reactivity of nZVI embedded into supermacroporous cryogels for highly efficient Cr(VI) and total Cr removal from aqueous solution," *Chemosphere*, vol. 199, pp. 232–242, 2018.

[2] H. W. Zou, E. D. Hu, S. Y. Yang, L. Gong, and F. He, "Chromium(VI) removal by mechanochemically sulfidated zero valent iron and its effect on dechlorination of trichloroethene as a co-contaminant," *Science of the Total Environment*, vol. 650, pp. 419–426, 2019.

[3] M. Bigalke, A. Ulrich, A. Rehmus, and A. Keller, "Accumulation of cadmium and uranium in arable soils in Switzerland," *Environmental Pollution*, vol. 221, pp. 85–93, 2017.

[4] D. D. Huang, G. C. Wang, and Z. M. Shi, "Removal of hexavalent chromium in natural groundwater using activated carbon and cast iron combined system," *Journal of Cleaner Production*, vol. 165, pp. 667–676, 2017.

[5] F. Obiri-Nyarko, S. J. Grajales-Mesa, and G. Malina, "An overview of permeable reactive barriers for _in situ_ sustainable groundwater remediation," *Chemosphere*, vol. 111, pp. 243–259, 2014.

[6] A. A. Alqadami, M. Naushad, M. A. Abdalla, T. Ahamad, Z. A. Alothman, and S. M. Alshehri, "Synthesis and characterization of Fe_3O_4@TSC nanocomposite: highly efficient removal of toxic metal ions from aqueous medium," *Rsc Advances*, vol. 6, no. 27, pp. 22679–22689, 2016.

[7] M. Villacis-Garcia, M. Villalobos, and M. Gutierrez-Ruiz, "Optimizing the use of natural and synthetic magnetites with very small amounts of coarse Fe(0) particles for reduction of aqueous Cr(VI)," *Journal of Hazardous Materials*, vol. 281, pp. 77–86, 2015.

[8] B. Dhal, H. N. Thatoi, N. N. Das, and B. D. Pandey, "Chemical and microbial remediation of hexavalent chromium from contaminated soil and mining/metallurgical solid waste: a review," *Journal of Hazardous Materials*, vol. 250, pp. 272–291, 2013.

[9] E. Kelepertzis, "Investigating the sources and potential health risks of environmental contaminants in the soils and drinking waters from the rural clusters in Thiva area (Greece)," *Ecotoxicology and Environmental Safety*, vol. 100, pp. 258–265, 2014.

[10] X. L. Liu, H. W. Pang, X. W. Liu, Q. Li, and N. Zhang, "Orderly porous covalent organic frameworks-based materials: superior adsorbents for pollutants removal from aqueous solutions," *The Innovation*, vol. 2, no. 1, p. 100076, 2021.

[11] B. W. Hu, Y. J. Ai, J. Jin et al., "Efficient elimination of organic and inorganic pollutants by biochar and biochar-based materials," *Biochar*, vol. 2, no. 1, pp. 47–64, 2020.

[12] D. Mallants, L. Diels, and L. Bastiaents, "Removal of uranium and arsenic from groundwater using six different reactive materials: assessment of removal efficiency," in *Uranium in the Aquatic Environment*, pp. 561–568, Springer, 2002.

[13] H. Zhou, J. Xu, and S. Lv, "Removal of cadmium in contaminated kaolin by new-style electrokinetic remediation using array electrodes coupled with permeable reactive barrier," *Separation and Purification Technology*, vol. 239, p. 116544, 2020.

[14] U. Kumarasinghe, K. Kawamoto, and T. Saito, "Evaluation of applicability of filling materials in permeable reactive barrier (PRB) system to remediate groundwater contaminated with Cd and Pb at open solid waste dump sites," *Process Safety and Environmental Protection*, vol. 120, no. 3, pp. 118–127, 2018.

[15] A. Kubier, R. T. Wilkin, and T. Pichler, "Cadmium in soils and groundwater: a review," *Applied Geochemistry*, vol. 108, p. 104388, 2019.

[16] R. W. Puls, C. J. Paul, and R. M. Powell, "The application of in situ permeable reactive (zero-valent iron) barrier technology for the remediation of chromate-contaminated groundwater: a field test," *Applied Geochemistry*, vol. 14, no. 8, pp. 989–1000, 1999.

[17] P. Y. Li, Y. Zhang, X. G. Gao, J. H. Song, and H. Dong, "Overview of maifanshi: its physichemical properties and nutritious function in drinking water," *Environmental Science & Technology*, vol. 31, pp. 63–66, 2008.

[18] W. Zhang, Y. Guo, Z. Pan, Y. Li, and H. Zeng, "Remediation of uranium-contaminated groundwater using the permeable reactive barrier technology coupled with hydroxyapatite-coated quartz sands," *Fresenius Environmental Bulletin*, vol. 27, no. 5, pp. 2703–2716, 2018.

[19] J. T. Gao, X. L. Zhang, and J. Yu, "Cr(VI) removal performance and the characteristics of microbial communities influenced by the core-shell maifanite/ZnAl-layered double hydroxides (LDHs) substrates for chromium-containing surface water," *Biochemical Engineering Journal*, vol. 160, p. 107625, 2020.

[20] B. Gu, D. B. Watson, and L. Wu, "Microbiological characteristics in a zero-valent iron reactive barrier," *Environmental monitoring and assessment*, vol. 77, no. 3, pp. 293–309, 2002.

[21] W. Teng, Z. F. Meng, and X. Ting, "Different adsorption modes and mechanisms of modified bentonite for phenol and phenanthrene," *Journal of Soil*, vol. 55, no. 3, pp. 683–694, 2018.

[22] N. Kang, N. Zhu, and W. Guo, "Efficient debromination of Tetrabromobisphenol A (TBBPA) by Au/ derived from bioreduction precious metals," *Chemical Engineering Journal*, vol. 334, pp. 99–107, 2018.

[23] S. Chang, H. Fu, X. Wu et al., "Batch and fixed-bed column studies for selective removal of cesium ions by compressible Prussian blue/polyurethane sponge," *Rsc Advances*, vol. 8, no. 64, pp. 36459–36467, 2018.

[24] Y. H. Yoon, J. H. Nelson, J. Lara, C. Kamel, and D. Fregeau, "A theoretical model for respirator cartridge service life for binary systems: application to acetone/styrene mixtures," *American Industrial Hygiene Association journal*, vol. 53, no. 8, pp. 493–502, 1992.

[25] O. Hamdaoui, "Dynamic sorption of methylene blue by cedar sawdust and crushed brick in fixed bed columns," *Journal of Hazardous Materials*, vol. 138, no. 2, pp. 293–303, 2006.

[26] P. Wu, W. Wu, and S. Li, "Removal of Cd^{2+} from aqueous solution by adsorption using Fe-montmorillonite," *Journal of hazardous materials*, vol. 169, no. 1-3, pp. 824–830, 2009.

[27] Y. Ma, W. J. Liu, and N. Zhang, "Polyethylenimine modified biochar adsorbent for hexavalent chromium removal from the aqueous solution," *Bioresource technology*, vol. 169, pp. 403–408, 2014.

[28] J. Liu, D. Wang, and L. Gao, "Synergism between cerium nitrate and sodium dodecylbenzenesulfonate on corrosion of AA5052 aluminium alloy in 3 wt.% NaCl solution," *Applied Surface Science*, vol. 389, pp. 369–377, 2016.

[29] S. Bilardi, P. S. Calabro, S. Care, N. Moraci, and C. Noubactep, "Improving the sustainability of granular iron/pumice systems for water treatment," *Journal of Environmental Management*, vol. 121, pp. 133–141, 2013.

[30] N. Gupta and T. C. Fox, "Hydrogeologic modeling for permeable reactive barriers," *Journal of hazardous materials*, vol. 68, no. 1-2, pp. 19–39, 1999.

[31] C. Sun, X. Wu, H. Meng, X. Xu, J. Xu, and X. Zhang, "Surface modification with EDTA molecule: a feasible method to enhance the adsorption property of ZnO," *Journal of Physics and Chemistry of Solids*, vol. 75, no. 6, pp. 726–731, 2014.

[32] S. A. Chattanathan, T. P. Clement, S. R. Kanel, M. O. Barnett, and N. Chatakondi, "Remediation of uranium-contaminated groundwater by sorption onto hydroxyapatite derived from catfish bones," *Water Air and Soil Pollution*, vol. 224, no. 2, 2013.

[33] K. Z. Setshedi, M. Bhaumik, M. S. Onyango, and A. Maity, "Breakthrough studies for Cr(VI) sorption from aqueous solution using exfoliated polypyrrole-organically modified montmorillonite clay nanocomposite," *Journal of Industrial and Engineering Chemistry*, vol. 20, no. 4, pp. 2208–2216, 2014.

[34] X. L. Zhang, Y. K. Dou, and C. G. Gao, "Removal of Cd(II) by modified maifanite coated with Mg-layered double hydroxides in constructed rapid infiltration systems," *Science of the Total Environment*, vol. 685, pp. 951–962, 2019.

[35] R. M. Jimenez and R. M. Solache, "Sorption behavior of fluoride ions from aqueous solutions by hydroxyapatite," *Journal of Hazardous Materials*, vol. 180, no. 1-3, pp. 297–302, 2010.

[36] C. Mahendra, P. M. S. Sai, C. A. Babu, K. Reyathy, and K. K. Rajan, "Analysis and modeling of fixed bed sorption of cesium by AMP-PAN," *Journal of Environmental Chemical Engineering*, vol. 3, no. 3, pp. 1546–1554, 2015.

[37] A. O. Akeem and G. Mustafa, "Fixed-bed column sorption of borate onto pomegranate seed powder-PVA beads: a response surface methodology approach," *Toxicological & Environmental Chemistry*, vol. 96, no. 6, pp. 837–848, 2014.

[38] A. O. Akeem, O. A. Edith, and G. Mustafa, "Pyrochar/AgBr-derived from discarded chewing gum for decontamination of trichlorophenol via fixed-bed adsorption system," *Chemical Engineering Communications*, vol. 208, no. 2, pp. 220–232, 2021.

[39] K. S. Wang, M. C. Wei, T. H. Peng et al., "Treatment and toxicity evaluation of methylene blue using electrochemical oxidation, fly ash adsorption and combined electrochemical oxidation-fly ash adsorption," *Journal of Environmental Management*, vol. 91, no. 8, pp. 1778–1784, 2010.

[40] Y. L. Zhu, X. Y. Hea, J. L. Xu et al., "Insight into efficient removal of Cr(VI) by magnetite immobilized with *Lysinibacillus* sp. JLT12: Mechanism and performance," *Chemosphere*, vol. 262, p. 127901, 2021.

[41] H. H. Wang, H. Guo, N. Zhang, Z. S. Chen, B. W. Hu, and X. K. Wang, "Enhanced photoreduction of U(VI) on C3N4by Cr(VI) and bisphenol A: ESR, XPS, and EXAFS Investigation," *Environmental Science & Technology*, vol. 53, no. 11, pp. 6454–6461, 2019.

[42] M. Q. Qiu, Z. Q. Liu, S. Q. Wang, and B. W. Hu, "The photocatalytic reduction of U(VI) into U(IV) by ZIF-8/g-C_3N_4 composites at visible light," *Environmental Research*, vol. 196, p. 110349, 2021.

[43] P. Mitra, D. Sarkar, S. Chakrabarti, and B. K. Dutta, "Reduction of hexa-valent chromium with ZVI: batch kinetic studies and rate model," *Chemical Engineering Journal*, vol. 171, no. 1, pp. 54–60, 2011.

[44] B. A. Manning, M. L. Hunt, C. Amrhein, and J. A. Yarmoff, "Arsenic(III) and arsenic(V) reactions with zerovalent iron corrosion products," *Environmental Science & Technology*, vol. 36, no. 24, pp. 5455–5461, 2002.

[45] Y. Y. Shen, R. L. Yang, Y. Liao, J. Ma, H. Mao, and S. L. Zhao, "Tannin modified aminated silica as effective absorbents for removal of light rare earth ions in aqueous solution," *Desalination and water treatment*, vol. 57, no. 39, pp. 18529–18536, 2016.

[46] G. Bartzas and K. Komnitsas, "Solid phase studies and geochemical modelling of low-cost permeable reactive barriers," *Journal of Hazardous Materials*, vol. 183, no. 1-3, pp. 301–308, 2010.

[47] A. N. Shabalala, S. O. Ekolu, S. Diop, and F. Solomon, "Pervious concrete reactive barrier for removal of heavy metals from acid mine drainage – column study," *Journal of Hazardous Materials*, vol. 323, pp. 641–653, 2017.